

Ab initio Study of the Electronic Structure of Zinc Oxide and its Ions, ZnO^{0,±}. Ground and Excited States

Constantine N. Sakellaris, Aristotle Papakondylis,* and Aristides Mavridis*

Department of Chemistry, Laboratory of Physical Chemistry, National and Kapodistrian University of Athens, P.O. Box 64004, Zografou, Athens 157 10, Greece

Received: May 25, 2010; Revised Manuscript Received: July 13, 2010

The species ZnO and ZnO[±] have been studied by variational multireference and coupled-cluster [RCCSD(T)] methods employing augmented basis sets of quintuple cardinality. Full potential energy curves are reported for 13, 10, and 2 bound states of ZnO, ZnO⁺, and ZnO⁻, respectively. All our results are in excellent agreement with existing experimental findings.

1. Introduction

It is well-known that first row transition metal diatomic oxides, MO, M = Sc (Z = 21) – Cu (Z = 29), have very complicated spectra reflecting their entangled electronic structure, a real challenge for experimentalists and theoreticians alike.^{1–4} Zinc, Zn (Z = 30), the next element to Cu, is an important element because of its significant role in many enzymes essential to life,⁵ while its oxide is lately considered a compound of technological interest. Work on the electronic structure of the diatomic oxide ZnO and its ions, either experimental or theoretical, is not very extended. Suffice to say that the accurate bond length of the X¹Σ⁺ state of ZnO has been experimentally determined only very recently by Zack et al.⁶ through pure rotational spectroscopy. In ref 6 a condensed literature review on ZnO is also given. To facilitate the reader and for reasons of comparison and completeness, Table 1 collects all previous data on ZnO both experimental and theoretical.

From Table 1 it can be seen that the most reliable calculations so far are those of Bauschlicher and Partridge,¹⁸ of Harrison et al.,¹⁹ and of Peterson et al.²⁰ These workers examined the (X¹Σ⁺, ³Π)^{18,20} and (X¹Σ⁺, ³Π, ³Σ⁺)¹⁹ states of ZnO, using coupled-cluster (RCCSD(T))^{18–20} and multireference variational methods (MRCI),²⁰ and basis sets of similar size;^{18,19} see footnotes of Table 1. Peterson and co-workers²⁰ employed aug-cc-pVnZ/O aug-cc-pVnZ-PP/Zn (n = D, T, Q, 5) basis sets, where the PP sets include Stuttgart small-core relativistic pseudopotentials adjusted to multiconfigurational Dirac–Hartree–Fock reference data. They report^{18–20} dissociation energies (*D*₀), bond distances (*r*_e), harmonic frequencies (*ω*_e), anharmonic corrections (*ω*_{e*x*e}), dipole moments (*μ*_e) and separation terms (*T*_e).

The most recent theoretical work on ZnO is that of Bourghdiri et al.,²¹ who calculated potential energy curves (PEC) for three bound (X¹Σ⁺, ³Π, ¹Π) and two repulsive (³Σ⁻, ¹Δ) states of ZnO, at the CCSD(T) and MRCI levels using Stuttgart small-core pseudopotentials for both atoms. No numerical results are given explicitly in ref 21 for the ¹Π state.

Experimental results on ZnO⁺ are limited to a dissociation energy, *D*₀⁰ = 1.67 ± 0.05 eV,¹⁰ and an ionization energy IE(ZnO) = 9.34 ± 0.02 eV,¹⁰ the latter being very close to zinc's ionization energy, IE(Zn) = 9.394 eV.²²

We are aware of only one theoretical publication on ZnO⁺ by Harrison et al.,¹⁹ who reported *r*_e, *D*₀, *ω*_e, and *T*₀ values of the X²Π and ²Σ⁺ states at the RCCSD(T)/[7s6p4d3f_{2g}/Zn, 6s5p4d3f₀] level of theory.

Concerning now the ZnO⁻ anion the following parameters have been determined experimentally for the X²Σ⁺ state: *r*_e (indirectly obtained from refs 6 and 14) = 1.753 Å, *D*₀ = 2.24 ± 0.05 eV,¹³ *ω*_e = 625 ± 40¹³ and 650 ± 50¹⁴ cm⁻¹, and the adiabatic electron affinity of ZnO, EA = 2.087 ± 0.008 eV.^{13,14} Theoretical results on ZnO⁻ (*D*₀, *r*_e, *ω*_e) at the RCCSD(T) level are reported by Bauschlicher and Partridge (X²Σ⁺)¹⁸ and Harrison et al. (X²Σ⁺, ²Π).¹⁹

Presently we investigate the structure and bonding of ZnO, and ZnO[±] by multireference (MRCI) and coupled cluster [RCCSD(T)] methods combined with extensive basis sets. In particular, we have constructed full PECs for all singlets and triplets of ZnO stemming from the first four Zn(¹S, ³P) + O(³P, ¹D, ¹S) channels within an asymptotic energy range of 4.2 eV,²² a total of 19 states, 13 bound and 6 of repulsive nature. For the ions ZnO⁺ and ZnO⁻ we have constructed PECs for 10 and 2 bound states, respectively.

For all bound states we report total energies, binding energies, common spectroscopic constants (*r*_e, *ω*_e, *ω*_{e*x*e}, *α*_e), dipole moments, and energy separation.

2. Technical Details

For the Zn atom the augmented correlation consistent basis set of quintuple cardinality was used, aug-cc-pV5Z = (29s21p13d5f4g3h2i),²³ whereas for the O atom the corresponding basis set, aug-cc-pV5Z = (15s9p5d4f3g2h)²⁴ was employed. Both sets were generally contracted to [10s9p7d5f4g3h2i]_{Zn} 7s6p5d4f3g2h_O] = A5ζ a total of 329 spherical Gaussians.

Two methods of calculation have been followed, the complete active space self-consistent field (CASSCF) + singles + double replacements (CASSCF + 1 + 2 = MRCI), and the restricted coupled-cluster + singles + doubles + quasi-perturbative triples [RCCSD(T)].²⁵ In the MRCI calculations the reference wave functions for ZnO, ZnO⁺, and ZnO⁻ were defined by distributing 6 [4s²(Zn) + 2p⁴(O)], 5 [4s¹(Zn⁺) + 2p⁴(O)], and 7 [4s²(Zn) + 2p⁵(O⁻)] electrons, respectively, to 7 orbitals [1(4s_{Zn}) + 3(4p_{Zn}) + 3(2p_O)]. Valence internally contracted (ic)²⁶ MRCI wave functions were calculated through single + double excitations out of the reference spaces, including, however, the 3d¹⁰ and 2s² electrons of Zn and O. The state average approach with

* To whom correspondence should be addressed. E-mail: mavridis@chem.uoa.gr (A. M.), papakondylis@chem.uoa.gr (A. P.).

TABLE 1: Previous Experimental and Theoretical Results of $^{64}\text{Zn}^{16}\text{O}^a$

experiment						
state	D_0	r_e	ω_e	$\omega_e x_e$	T_0	
?	$<2.86^b$					
?			808 ^c			
?	$\geq 2.8 \pm 0.2^d$					
$X^1\Sigma^+$	1.61 ± 0.04^e					
$X^1\Sigma^+$	$\leq 2.3^f$					
$X^1\Sigma^+$			769.2 ^g			
$X^1\Sigma^+$			805 ± 40^h			
$a^3\Pi$	1.36^i					0.25^h
$X^1\Sigma^+$		R^j	720 ± 20^j			
$a^3\Pi$		1.831 ± 0.005^{jk}	550 ± 20^j			0.302 ± 0.1^j
$A^1\Pi$		1.828 ± 0.005^{jk}	590 ± 20^j	3		0.611 ± 0.1^j
$b^3\Sigma^+$		1.791 ± 0.005^{jk}	560 ± 20^j			1.865 ± 0.1^j
$X^1\Sigma^{+l}$			770 ± 40			
$a^3\Pi^l$		1.850	540 ± 80			0.305 ± 0.015
$A^1\Pi^l$		1.838	600 ± 80			0.615 ± 0.019
$X^1\Sigma^{+m}$		1.7047	738	4.88		
$a^3\Pi^m$		1.8436	562	4.76		
theory						
state	D_0	r_e	ω_e	$\omega_e x_e$	μ_e	T_e
$1^1\Sigma^+ n$	0.66	1.711	725		6.33	
$X^1\Sigma^+ o$		1.733	690		5.374	0.0
$3^1\Pi^o$		1.873	525		2.613	0.215 ^p
$3^3\Sigma^+ o$		1.818	561		3.124	1.689 ^p
$3^3\Sigma^- o$		4.576	15		0.075	1.337 ^p
$X^1\Sigma^+ q$	1.63	1.719	727.2	5.83		0.0
$3^1\Pi^q$	1.38	1.857	566.6	4.36		0.26
$X^1\Sigma^+ r$	3.54	1.715	741		5.49	0.0
$3^1\Pi^r$	1.31	1.850	577		2.62	0.35(= T_0)
$3^3\Sigma^+ r$	3.87	1.801	596		3.11	1.83(= T_0)
$X^1\Sigma^+ s$	3.45 ^t	1.712	726 ^t	4.1	5.33 ^u	0.0
$3^1\Pi^s$	1.26 ^v	1.835	586 ^v	5.4		0.238(= T_0)
$X^1\Sigma^+ w$	3.54	1.689	766	6.04	~ 5.59	0.0
$3^1\Pi^w$	1.10	1.872	590	4.76	~ 2.80	0.275

^a Dissociation Energies D_0 (eV), Bond Distances r_e (Å), Harmonic frequencies and Anharmonicity Corrections, ω_e , $\omega_e x_e$ (cm⁻¹), Dipole Moments μ_e (D), and Separation Energies T_0 (eV). ^b Reference 7. Mass spectroscopic measurements, D_{298}^0 value. ^c Reference 8. IR, Raman, and visible spectroscopic study of Zn + O₃ in Ar and N₂ matrices. ^d Reference 9. Chemiluminescence spectroscopy of Zn + N₂O. ^e Reference 10. Guided ion-beam mass spectroscopy, D_0^0 value. ^f Reference 11. High temperature mass spectrometry, D_0^0 value. ^g Reference 12. Fourier transform IR spectroscopy. ^h Reference 13. Negative ion photoelectron spectroscopy (PES). ⁱ Reference 13. Indirectly obtained through the D_0^0 value of ref 10. ^j Reference 14. Anion PES. $r_e = R$ (not determined). ^k Reference 14. With respect to $R (= r_e) = 1.7047$ of ref 6. ^l Reference 15. Vibrationally resolved PES of ZnO⁻. ^m Reference 6. Pure rotational spectroscopy. It is also given $\alpha_e = 3.81 \times 10^{-3}$ cm⁻¹, and $D_0 = 78.6$ kcal/mol obtained through the approximate formula $D_e \approx \omega_e^2/4\omega_e x_e$ but with respect to Zn(1S) + O(1D). ⁿ Reference 16. CISD/SEFIT pseudopotentials + [6s5p3d/zn4s3p1d/o]. ^o Reference 17. QCISD/[6-311 ++ G(d,f)]. ^p Reference 17. T_e obtained at the QCISD(T)//[6-311 ++ G(2d,2f)] level. $E_{\text{QCISD(T)}(X^1\Sigma^+)} = -1853.143193$ E_h. ^q Reference 18. CCSD(T)/[ANO-7s6p4d3f2g/zn aug-cc-PVQZ/o]. D_0 values with respect to the ground state atoms Zn(1S) + O(3P). ^r Reference 19. RCCSD(T)/[7s6p4d3f2g/zn6s5p4d3f/o] + scalar relativistic corrections at the CISD//RCCSD(T) level. D_0 values with respect to Zn(1S) + O(1D), Zn(1S) + O(3P), and Zn(3P) + O(3P) for $X^1\Sigma^+$, $3^1\Pi_1$, and $3^3\Sigma^+$ states, respectively. ^s Reference 20. MRCI+Q/[aug-cc-pVnZ/aug-cc-pVnZ-pp/zn] CBS results (n = D,T, Q, 5). ^t Reference 20. Corrections for the 1s² and 3s²3p⁶ electrons of O and Zn included. D_0 with respect to Zn(1S) and O(1D). ^u Reference 20. μ_e calculated at the RCCSD(T)/aug-cc-pVTZ level. ^v Reference 20. Corrections for the 1s² and 3s²3p⁶ electrons of O and Zn included. D_0 with respect to Zn(1S) and O(3P). ^w Reference 21. Valence CCSD(T)/Stuttgart small-core pseudopotentials for both O and Zn, but the rest of basis sets are not clearly specified.

equal weights was applied to the last 9 and 7 states of ZnO and ZnO⁺, respectively. All calculations were done under C_{2v} constraints. Valence icMRCI spaces range from $\sim 4 \times 10^6$ (ZnO⁺) to $\sim 6 \times 10^6$ (ZnO⁻) configuration functions.

Scalar relativistic effects for the first 4, 3, and 2 states of ZnO, ZnO⁺, and ZnO⁻ species were obtained through the fifth order Douglas–Kroll–Hess (DKH) method.^{27,28,31} At the fifth order energies are practically converged, although calculated properties change only slightly after the second order. For the DKH calculations the Zn basis set was recontracted according to ref 23, whereas the O basis set was left uncontracted.

Basis set superposition errors (BSSE) calculated as usual by the counter-poise method are quite small, so are not considered any further. For instance, at the MRCI/A5 ζ level the BSSE for the $X^1\Sigma^+$ state of ZnO is ~ 0.20 kcal/mol.

To ameliorate size nonextensivity errors (SNE) that are significant, for instance, ~ 24 mE_h for the $X^1\Sigma^+$ state of ZnO, the Davidson correction (+Q)²⁹ was applied. The multireference averaged coupled cluster pair functional (ACPF)³⁰ approach was also used for the first 4, 3, and 2 lowest states of ZnO, ZnO⁺, and ZnO⁻, respectively. At the MRCI+Q and ACPF levels the SNE for the $X^1\Sigma^+$ state of ZnO reduces to 5.6 and 0.71 mE_h, respectively.

All calculations were performed with the MOLRO 2006.1 package.³¹

3. Results and Discussion

A. ZnO. Numerical results of the first 13 bound states of ZnO are collected in Table 2, and Figure 1 displays PECs of

TABLE 2: Total Energies E (E_h), Bond Distances r_e (\AA), Dissociation Energies D_0 (eV), Harmonic Frequencies and Anharmonicity Corrections, ω_e and $\omega_e x_e$ (cm^{-1}), Rotational-Vibrational Coupling Constants $\alpha_e \times 10^3$ (cm^{-1}), Dipole Moments μ_e (D), and Energy Separations T_0 (eV) of the $^{64}\text{Zn}^{16}\text{O}$ Molecule

method ^a	$-E$	r_e	D_0^b	ω_e	$\omega_e x_e$	α_e	$\langle \mu \rangle / \mu_{\text{FF}}^c$	T_0
X $^1\Sigma^+ d$								
MRCI	1853.38524	1.720	3.60 (1.63)	728	5.0	3.7	5.42/5.68	0.0
MRCI+Q	1853.4350	1.715	3.59 (1.63)	740	5.1	3.7	/5.70	0.0
MRCI+DKH	1869.90715	1.709	3.51 (1.55)	733	4.9	3.8	5.34/5.54	0.0
MRCI+DKH+Q	1869.9578	1.703	3.50 (1.54)	744	5.0	3.8	/5.52	0.0
ACPF	1853.43566	1.717	3.64 (1.67)	737	4.9	3.7	5.21/5.54	0.0
ACPF+DKH	1869.95851	1.705	3.55 (1.58)	742	4.9	3.8	5.12/5.41	0.0
RCCSD(T)	1853.45658	1.712	3.76 (1.60)	730	3.8	4.2	/5.32	0.0
RCCSD(T) + DKH	1869.98014	1.700	3.67 (1.51)	737	3.6	4.5	/5.19	0.0
Expt.		1.7047 ^e	3.568 (1.61 \pm 0.04) ^f	738 ^e	4.88 ^e	3.81 ^e		
a $^3\Pi^g$								
MRCI	1853.37699	1.853	1.42	587	4.0	3.4	2.61/2.69	0.22
MRCI+Q	1853.4240	1.849	1.34	584	4.1	3.5	/2.67	0.29
MRCI+DKH	1869.89788	1.844	1.31	586	4.1	3.6	2.56/2.62	0.24
MRCI+DKH+Q	1869.9460	1.840	1.23	582	4.3	3.7	/2.59	0.31
ACPF	1853.42431	1.852	1.37	582	4.5	3.6	2.62/2.68	0.30
ACPF+DKH	1869.94632	1.843	1.26	579	4.5	3.7	2.56/2.60	0.32
RCCSD(T)	1853.44590	1.848	1.32	577	4.4	3.7	/2.54	0.28
RCCSD(T) + DKH	1869.96881	1.839	1.21	574	4.7	3.9	/2.46	0.30
Expt.		1.8436 ^e	1.308 \pm 0.14 ^h 1.305 \pm 0.06 ^j	562.0 ^e	4.76 ^e	4.016 ^e		0.302 \pm 0.1 ⁱ 0.305 \pm 0.015 ^k
A $^1\Pi'$								
MRCI	1853.36832	1.846	3.16	611	3.2	3.0	2.60/2.75	0.45
MRCI+Q	1853.4149	1.841	3.05	612	3.2	3.0	/2.74	0.54
MRCI+DKH	1869.88836	1.836	3.02	614	3.3	3.1	2.56/2.69	0.50
MRCI+DKH+Q	1869.9359	1.830	2.91	615	3.3	3.1	/2.68	0.59
ACPF	1853.41529	1.843	3.09	611	3.3	3.1	2.61/2.75	0.55
ACPF+DKH	1869.93639	1.832	2.96	614	3.3	3.2	2.56/2.69	0.59
Expt.		1.838 ^k 1.828 \pm 0.005 ^m		590 \pm 20 ^j	3 ⁱ			0.611 \pm 0.1 ⁱ 0.615 \pm 0.019 ^k
b $^3\Sigma^+ n$								
MRCI	1853.29831	1.789	3.05	646	10.7	4.6	2.63/3.22	2.36
MRCI+Q	1853.3602	1.780	3.44	656	8.5	4.3	/3.16	2.03
MRCI+DKH	1869.84463	1.806	3.63	585	3.5	3.6	3.04/3.13	1.69
MRCI+DKH+Q	1869.8923	1.797	3.72	589	3.5	3.7	/3.10	1.78
ACPF	1853.37333	1.808	3.71	588	3.5	3.6	2.94/3.12	1.69
ACPF+DKH	1869.89205	1.801	3.69	587	3.5	3.7	2.94/3.12	1.80
RCCSD(T)	1853.39418	1.799	3.76	591	3.4	3.6	/2.94	1.69
RCCSD(T) + DKH	1869.91369	1.792	3.76	591	3.4	3.7	/2.96	1.80
Expt.		1.791 \pm 0.005 ^o		560 \pm 20 ^j				1.865 \pm 0.1 ⁱ
c $^3\Pi^n$								
MRCI	1853.25309	2.523	1.84	327	1.2	0.1	1.85/2.16	3.57
MRCI+Q	1853.3054	2.482	1.97	336	1.3	0.0	/2.15	3.50
B $^1\Sigma^+ n$								
MRCI	1853.23120	1.763	1.24	707	12.7	6.4	2.94/2.89	4.19
MRCI+Q	1853.2970	1.741	1.72	736	7.6	4.4	/3.45	3.75
C $^1\Pi^n$								
MRCI	1853.22295	3.033	1.01	281	2.3	-1.3	1.85/2.16	4.39
MRCI+Q	1853.2747	2.971	1.13	251	0.6	-0.7	/2.15	4.33
d $^3\Sigma^+ p$								
MRCI	1853.21839	1.837	2.85	595	7.2	3.9	2.92/2.97	4.53
MRCI+Q	1853.2752	1.834	3.08	604	7.3	4.0	/2.89	4.34
e $^3\Delta^n$								
MRCI	1853.21431	1.860	0.77	502	-1.6	2.6	2.38/2.65	4.69
MRCI+Q	1853.2697	1.846	0.98	561	5.0	3.7	/2.71	4.49
f $^3\Sigma^- n$								
MRCI	1853.20722	1.892	0.58	478	-7.7	1.9	2.01/2.28	4.83
MRCI+Q	1853.2630	1.872	0.79	544	1.1	3.2	/2.41	4.67
D $^1\Sigma^- n$								
MRCI	1853.20258	1.941	0.48	405	10.9	8.3	1.52/1.58	4.95
MRCI+Q	1853.2593	1.895	0.71	467	8.6	6.5	/2.01	4.76
E $^1\Delta^n$								
MRCI	1853.19982	2.081	0.40	445	17.2	9.5	0.59/0.69	5.03
MRCI+Q	1853.2546	2.057	0.58	579	24.3	7.7	/0.81	4.90
F $^1\Sigma^+ g$								
MRCI	1853.16302	2.125	0.24	341	24.8	17.0	0.05/0.92	6.02
MRCI+Q	1853.2264	2.309	0.23	314	24.9	12.1	/0.73	5.65

^a +Q and DKH refer to Davidson correction and Douglas-Kroll-Hess scalar relativistic corrections of the 5th order, respectively. ^b D_0 ($= D_e - \omega_e/2 + \omega_e x_e/4$). ^c $\langle \mu \rangle$ calculated as an expectation value, μ_{FF} through the finite field approach; field strength 10^{-5} au. ^d D_0 with respect to Zn(¹S) + O(¹D); values in parentheses with respect to the ground state atoms Zn(¹S) + O(³P). ^e Reference 6. ^f Reference 10. 3.568 eV = 1.61 + $\Delta E_{\text{expt}}[\text{O}(\text{1D}) \leftarrow \text{O}(\text{3P})]$. ^g D_0 with respect to Zn(¹S) + O(³P). ^h $D_0 = 1.61 \pm 0.04^{10} - (0.302 \pm 0.1)^{14} = 1.308 \pm 0.14$ eV. ⁱ Reference 14. ^j $D_0 = 1.61 \pm 0.04^{10} - (0.305 \pm 0.015)^{15} = 1.305 \pm 0.05$ eV. ^k Reference 15. ^l D_0 with respect to Zn(¹S) and O(¹D). ^m Reference 14. $r_e = R(\text{X}^1\Sigma^+) + 0.123(5) = 1.70474 \text{ \AA} + 0.123(5) \text{ \AA}^{14} = 1.828 \pm 0.005 \text{ \AA}$. ⁿ D_0 with respect to Zn(³P)+O(³P). ^o Reference 14. $r_e = R + 0.086$. $R = 1.7047$ from ref 6. ^p D_0 with respect to Zn(³P) + O(¹D). ^q D_0 with respect to Zn(¹S) + O(¹S).

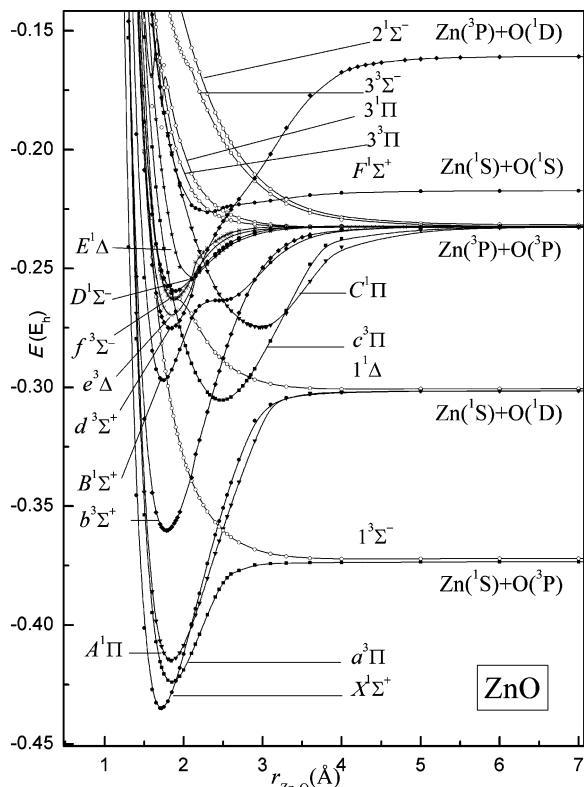


Figure 1. MRCI+Q/A5 ζ PECs of ZnO. All energies are shifted by +1853 E_h .

19 states at the MRCI+Q/A5 ζ level of theory. In what follows we discuss the manifold of bound states in ascending energy order.

$X^1\Sigma^+$. The ground state of ZnO, $X^1\Sigma^+$, correlates adiabatically to $Zn(^1S) + O(^1D)$. The leading equilibrium MRCI configuration functions and Mulliken distributions are (counting valence electrons only for simplicity)

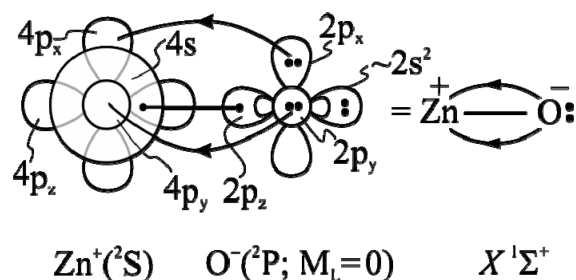
$$|X^1\Sigma^+\rangle \approx 0.90|1\sigma^2 2\sigma^2 1\pi_x^2 1\pi_y^2\rangle \\ 4s^{1.00} 4p_z^{0.09} 4p_x^{0.13} 4p_y^{0.13} /_{Zn} 2s^{1.86} 2p_z^{1.05} 2p_x^{1.84} 2p_y^{1.84} /_O$$

A total of near $0.65 e^-$ are transferred from Zn to the oxygen atom. The $4s^{1.00}$ distribution on Zn around equilibrium along with the strongly ionic character of ZnO dictates the valence-bond-Lewis (vbL) bonding diagram shown in Scheme 1 suggesting two weak $\pi(4p_{\pi}^{Zn} - 2p_{\pi}^O)$ bonds and a σ bond. This bonding picture is in complete conformity with the Mulliken distributions. Obviously the $3d^{10}$ electrons of Zn are completely irrelevant to the bonding, being well buried under the $4s^2$ distribution, the Hartree-Fock ratio of $4s$ to $3d$ radii being $\langle r_{4s} \rangle / \langle r_{3d} \rangle = 3.31$.³²

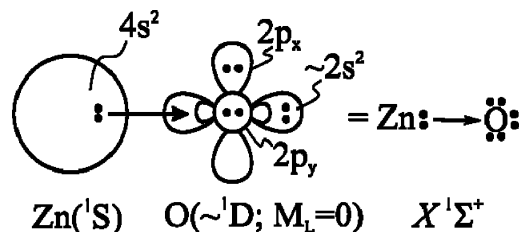
Stretching the two atoms apart, the $Zn^+ - O^-$ diabatic PEC suffers an avoided crossing near 3.0 \AA with the adiabatic PEC pertaining to $Zn(^1S) + O(^1D; M_L = 0)$ end fragments; see Figure 1. The corresponding vbL diagram is shown in Scheme 2.

Notice that the correct determinantal expansion of the $^1D(M_L = 0)$ term of the O atom is $|^1D; M_L = 0\rangle = (1/\sqrt{6})(2|p_x^2 p_y^2\rangle - |p_x^2 p_z^2\rangle - |p_y^2 p_z^2\rangle)$. It is interesting to mention that the full PEC of the $X^1\Sigma^+$ state can be constructed equally well at the RCCSD(T) level; as a matter of fact, the MRCI and RCCSD(T) PECs are, in essence, identical, strongly supporting the above bonding diagram. Moving away from equilibrium where the ionic bonding prevails, the dative bond nature takes over (vbL 2)

SCHEME 1



SCHEME 2



therefore the single reference RCCSD(T) approach traces accurately the potential curve.

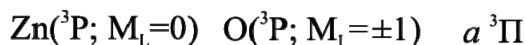
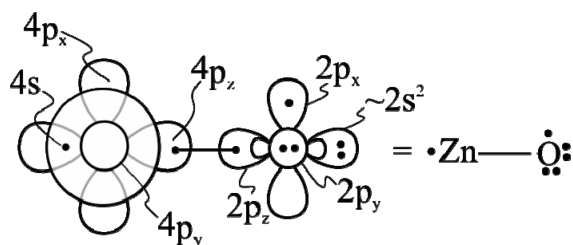
As can be seen from Table 1 the calculated bond distance is in excellent agreement with experiment in all methods of calculation, but after taking into account scalar relativistic effects. The bond distance decreases consistently by $\sim 0.01 \text{ \AA}$ in all methods and for all four lower states ($X^1\Sigma^+$, $a^3\Pi$, $A^1\Pi$, $b^3\Sigma^+$) when scalar relativity is included. Thus, our MRCI+DKH+Q (ACPF+DKH) $r_e = 1.703(1.705) \text{ \AA}$, as contrasted to the experimental value of 1.7047 \AA ,⁶ at the RCCSD(T)+DKH level r_e is underestimated by $\sim 0.005 \text{ \AA}$. Notice that scalar relativity is responsible for reducing the binding energy by $\sim 0.10\text{--}0.14 \text{ eV}$ in the first three lower states. With respect to the adiabatic atoms, $Zn(^1S) + O(^1D)$, the binding energy converges to $D_0 = 3.60 \pm 0.1 \text{ eV}$, the lower and the higher value corresponding to MRCI+DKH+Q and RCCSD(T)+DKH methods, respectively. The agreement with experiment, $D_0 = D_0$ [with respect to $Zn(^1S) + O(^3P)] + \Delta E[O(^1D) \leftarrow O(^3P)] = 1.61 \pm 0.04^{10} + 1.958^{22} = 3.568 \pm 0.04 \text{ eV}$, can be considered as quite satisfactory. Similar results for the D_0 of the $X^1\Sigma^+$ state have been obtained by the previous workers;^{19,20} see Table 1. As to the dipole moment, the finite field value, μ_{FF} , is bracketed between 5.2 and 5.5 D , with a recommended value $\mu_{FF} = 5.3 \pm 0.1 \text{ D}$;³³ see Table 2. Estimating the dipole moment by the relation $\mu_e = q \cdot r_e$, with q (Mulliken) = 0.65 and $r_e = 1.703 \text{ \AA}$, we get $\mu_e = 5.32 \text{ D}$ in pleasant agreement with the μ_{FF} value. No experimental value of the dipole moment of ZnO exists in the literature.

$a^3\Pi$. This is the first excited state of ZnO correlating adiabatically to the ground state atoms (Figure 1). It is clear that the $4s^2(Zn; ^1S) + 2s^2 2p^4(O; ^3P)$ distributions are not suitable for bond formation; at the most one expects a van der Waals-like interaction. The explanation of a relatively strong bond lies in the interaction of the $a^3\Pi$ and $c^3\Pi$ states, the latter correlating to $Zn(4s^1 4p^1; ^3P) + O(^3P)$, see Figure 1. The main equilibrium MRCI configuration and Mulliken populations of the $a^3\Pi$ state are

$$|a^3\Pi\rangle \approx 0.95|1\sigma^2 2\sigma^2 3\sigma^1 1\pi_x^1 1\pi_y^2\rangle \\ 4s^{1.07} 4p_z^{0.32} 4p_x^{0.02} 4p_y^{0.05} /_{Zn} 2s^{1.94} 2p_z^{1.64} 2p_x^{0.98} 2p_y^{1.92} /_O$$

The bonding can be described by the vbL diagram shown in Scheme 3.

SCHEME 3



A transfer of $\sim 0.6 e^-$ from the $(4s^1 4p^1)$ distribution to the singly occupied $2p_z$ orbital of the O atom is responsible for the σ bond (2σ orbital). The interaction of the $a^3\Pi$ and $c^3\Pi$ states occurs at $r \sim 2.7 \text{ \AA}$; at this point the populations of $4s$, $4p_z$, and $2p_z$ change drastically from ~ 2.0 , 0.0 , and $1.0 e^-$ at infinity to about 1.4 , 0.2 , and $1.4 e^-$, respectively, finally becoming ~ 1.1 , 0.3 , and $1.65 e^-$ at equilibrium.

Table 2 reveals that the calculated r_e is in excellent agreement with experiment, the largest discrepancy being -0.004 \AA at the RCCSD(T) level. The same can be said for the dissociation energy where the (recommended) $D_0 = 1.25 \text{ eV}$, as compared to the experimental numbers 1.308 ± 0.14 and $1.305 \pm 0.06 \text{ eV}$; see Table 2. The calculated energy separation $T_0(a^3\Pi - X^1\Sigma^+) = 0.31 \text{ eV}$ is also in complete agreement with experiment, $T_0 = 0.302 \pm 0.1$,¹⁴ or $0.305 \pm 0.015 \text{ eV}$.¹⁵ Finally the (finite field) dipole moment, smaller by $\sim 3 \text{ D}$ from that of the $X^1\Sigma^+$ state, is bracketed between 2.5 and 2.6 D . Our results are, in general, very similar to those of Harrison et al.¹⁹ and Peterson et al.,²⁰ but differ significantly from the results of Boughdiri et al.²¹ The fact that $\mu_e(X^1\Sigma^+) \cong 2 \cdot \mu_e(a^3\Pi)$ can be rationalized by the $4s 4p_z$ electron distribution on the back of the Zn atom in the $a^3\Pi$ state; compare vbL diagrams 1 and 2 to 3.

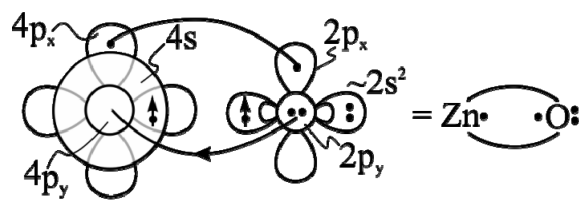
A¹Π. This is in essence the first theoretical report on the ¹Π state (but see below), the second excited state of ZnO, lying $\sim 0.6 \text{ eV}$ above the $X^1\Sigma^+$ and correlating adiabatically to $\text{Zn}(^1\text{S}) + \text{O}(^1\text{D})$; see Figure 1 and Table 2. Diabatically, however, the $A^1\Pi$ state correlates to $\text{Zn}(^3\text{P}) + \text{O}(^3\text{P})$, the result of a $C^1\Pi - A^1\Pi$ interaction near 3 \AA . *Mutatis mutandis* the situation is completely analogous to the $a^3\Pi$ state previously described: the leading MRCI equilibrium configuration and the corresponding Mulliken populations are identical to those of $a^3\Pi$, while the bonding is described by the vbL diagram 3 but with the $4s^1 - 2p_x^1$ electrons coupled into a singlet.

Our results, r_e , ω_e , $\omega_e x_e$, and T_0 are in excellent agreement with experiment at both MRCI+DKH+Q and ACPF+DKH levels. The recommended dissociation energy and (finite field) dipole moment are $D_0 = 3.00 \text{ eV}$ and $\mu_{\text{FF}} = 2.70 \text{ D}$; see Table 2. From the PEC of Figure 1 of reference²¹ we deduce that $r_e \approx 1.75 \text{ \AA}$, $D_e \approx 2.86 \text{ eV}$, and $T_e \approx 0.80 \text{ eV}$.

b³Σ⁺. The third excited state of ZnO is of ³Σ⁺ symmetry, located 1.80 eV higher and correlating to $\text{Zn}(4s^1 4p^1; ^3\text{P}) + \text{O}(^3\text{P})$; see Figure 1 and Table 2. Previous calculations are by Boldyrev and Simons,¹⁷ and Harrison et al.¹⁹ Our results are in practical agreement with those of ref.¹⁹ The main equilibrium configuration and Mulliken populations are given below

$$|b^3\Sigma^+\rangle \approx 0.89|1\sigma^2 2\sigma^1 3\sigma^1 1\pi_x^2 1\pi_y^2\rangle \\ 4s^{0.94} 4p_z^{0.19} 4p_x^{0.18} 4p_y^{0.18} /_{\text{Zn}} 2s^{1.93} 2p_z^{0.92} 2p_x^{1.79} 2p_y^{1.79} /_{\text{O}}$$

SCHEME 4



A total charge transfer of $0.50 e^-$ is observed from Zn to O. The bonding picture can be captured by the vbL diagram shown in Scheme 4.

The four electrons can be coupled into a triplet either in the σ or in the π frame; the diagram above indicates the former. We suggest a π singlet by following the populations of $4s$, $4p_\pi$, $2p_\pi$, and $2p_z$ from infinity to equilibrium: the $4s$ and $2p_z$ occupations change only slightly from 1.0 to 0.94 and 0.92 , respectively, whereas the $2p_\pi$ from 3.10 to 3.60 . Including the population of $4p_\pi(\text{Zn})$ at equilibrium, the total population of the π frame becomes 3.95 , equally shared as it should between π_x and π_y . On the other hand we can think the molecule as ionic, $\text{Zn}^+(^2\text{S}; 4s^1(\uparrow))\text{O}^-(^2\text{P}; 2p_z^1(\uparrow))$; certainly both pictures contribute to the bonding as in all three states $X^1\Sigma^+$, $a^3\Pi$, and $A^1\Pi$ previously discussed.

Compared to the experimental bond distance $r_e = 1.791 \pm 0.005 \text{ \AA}$ obtained indirectly,¹⁴ our calculated r_e is in very good agreement in all methods after including scalar relativity. The recommended $D_0 = 3.70 \text{ eV}$, using the mean value of MRCI+DKH+Q and ACPF+DKH results, while the RCCSD(T)+DKH number is slightly larger, $D_0 = 3.76 \text{ eV}$. Finally our recommended dipole moment is $\mu_{\text{FF}} = 3.1 \text{ D}$.

c³Π, B¹Σ⁺, C¹Π, e³Δ, f³Σ⁻, D¹Σ⁻, E¹Δ. All seven states correlate to $\text{Zn}(^3\text{P}) + \text{O}(^3\text{P})$, they are located within an MRCI+Q energy window of 1.37 eV ($= 32 \text{ kcal/mol}$), they are all bound with respect to $\text{Zn}(^3\text{P}) + \text{O}(^3\text{P})$ with binding energies ranging from 1.97 ($c^3\Pi$) to 0.58 eV ($E^1\Delta$), while their μ_{FF} dipole moments range from 0.70 ($E^1\Delta$) to 3.5 ($B^1\Sigma^+$) D at the MRCI+Q level; see Table 2 and Figure 1. Their leading MRCI configurations and total Mulliken charges on Zn (q_{Zn}) are tabulated below

$$|c^3\Pi\rangle \approx 0.89|1\sigma^2 2\sigma^1 3\sigma^2 1\pi_x^1 1\pi_y^2\rangle \quad (+0.31)$$

$$|B^1\Sigma^+\rangle \approx 0.63|1\sigma^2 2\sigma^1 3\sigma^1 1\pi_x^1 1\pi_y^2\rangle \\ -0.41|1\sigma^2 2\sigma^2(1\pi_x^1 1\pi_y^2 2\pi_y^1 + 1\pi_x^2 2\pi_x^1 1\pi_y^2)\rangle \quad (+0.48)$$

$$|C^1\Pi\rangle \approx 0.78|1\sigma^2 2\sigma^1 3\sigma^2 1\pi_x^1 1\pi_y^2\rangle (+0.15)$$

$$|e^3\Delta\rangle \approx 0.65|1\sigma^2 2\sigma^2(1\pi_x^1 2\pi_x^1 1\pi_y^2 - 1\pi_x^2 1\pi_y^2 2\pi_y^1)\rangle \quad (+0.27)$$

$$|f^3\Sigma^-\rangle \approx 0.63|1\sigma^2 2\sigma^2(1\pi_x^2 2\pi_x^1 1\pi_y^2 + 1\pi_x^1 1\pi_y^2 2\pi_y^1)\rangle \quad (+0.25)$$

$$|D^1\Sigma^-\rangle \approx 0.61|1\sigma^2 2\sigma^2(1\pi_x^1 1\pi_y^2 2\pi_y^1 - 1\pi_x^2 2\pi_x^1 1\pi_y^2)\rangle \quad (+0.19)$$

$$|E^1\Delta\rangle \approx 0.55|1\sigma^2 2\sigma^2(1\pi_x^2 1\pi_y^2 2\pi_y^1 - 1\pi_x^1 2\pi_x^1 1\pi_y^2)\rangle \\ -0.31|1\sigma^2 2\sigma^1 3\sigma^2 1\pi_x^1 1\pi_y^2\rangle \quad (+0.10)$$

F¹Σ⁺, d³Σ⁺. The $F^1\Sigma^+$ state correlates to the $\text{Zn}(^1\text{S}; 4s^2) + \text{O}(^1\text{S})$ channel, where ¹S is the second excited term of the O atom located experimentally²² (theoretically at the MRCI+Q supermolecule) 4.18 (4.25) eV above its ground ³P state. The leading equilibrium MRCI configurations and Mulliken atomic populations of the $F^1\Sigma^+$ state are

$$|F^1\Sigma^+\rangle \approx 0.451|1\sigma^22\sigma^23\sigma^2(1\pi_x^2 + 1\pi_y^2)\rangle - 0.391|1\sigma^23\sigma^21\pi_x^21\pi_y^2\rangle$$

$$4s^{1.22}4p_z^{0.15}4p_x^{0.20}4p_y^{0.20}/_{Zn}2s^{1.96}2p_z^{1.67}2p_x^{1.28}2p_y^{1.28}/_O$$

with a total Zn to O charge transfer of $\sim 0.20 e^-$. The 1S term of the O atom is described by the linear combination $|^1S; 2s^22p^4\rangle = (1/\sqrt{3})2s^2(2p_x^22p_z^2 + 2p_y^22p_z^2 + 2p_x^22p_y^2)$, or $4/3 = 1.33 e^-$ per $2p_i$ ($i = x, y, z$) atomic orbital. At equilibrium this distribution is practically maintained in the $2s$, $2p_x$, and $2p_y$ orbitals, while $\sim 0.30 e^-$ are transferred from the $(4s4p_z)^2$ hybrid on Zn to the $2p_z$ orbital of the O atom. This dative type of bonding is also corroborated by the composition of the MRCI natural orbitals, $2\sigma \approx (0.51)4s^{Zn} - (0.78)2p_z^O$ and $3\sigma \approx (0.94)4s^{Zn} + (0.60)2p_z^O$. At the MRCI+Q level $r_e = 2.31 \text{ \AA}$ and $D_0 = 0.23 \text{ eV}$ ($= 5.3 \text{ kcal/mol}$), with $\mu_{FF} \approx 0.7 \text{ D}$; see Table 2.

The $d^3\Sigma^+$ state correlates to the first excited states of $Zn(^3P; M_L = 0)$ and $O(^1D; M_L = 0)$ and it is strongly bound with respect to this channel, $D_0 = 3.08 \text{ eV}$ at $r_e 1.834 \text{ \AA}$, with $\mu_{FF} = 2.9 \text{ D}$ at the MRCI+Q level of theory. Its leading MRCI configurations and Mulliken densities are

$$|d^3\Sigma^+\rangle \approx 0.651|1\sigma^22\sigma^2(1\pi_x^21\pi_y^2 + 1\pi_x^21\pi_y^22\pi_z^2)\rangle$$

$$4s^{0.52}4p_z^{0.08}4p_x^{0.53}4p_y^{0.53}/_{Zn}2s^{1.93}2p_z^{1.44}2p_x^{1.45}2p_y^{1.45}/_O$$

with a total Zn to O e^- transfer of $\sim 0.30 e^-$. The bonding is caused by a $\sim 0.40 e^-$ transfer from the $(4s4p_z)^1$ hybrid on Zn to the $2p_z$ orbital of the oxygen atom. Recall that at infinity the $M_L = 0$ component of the 1D term of the O atom is a linear combination of three determinants, namely, $|^1D; M_L = 0\rangle = (1/\sqrt{6})2s^2[(2 \times)2p_x^22p_y^2 - 2p_x^22p_z^2 - 2p_y^22p_z^2]$. Finally six of the states, $1^3\Sigma^-, 1^1\Delta$, and $(3^1\Pi, 3^3\Pi, 3^3\Sigma^-, 2^1\Sigma^-)$ correlating to $Zn(^1S) + O(^3P)$, $Zn(^1S) + O(^1D)$, and $Zn(^3P) + O(^3P)$, respectively are of repulsive nature; see Figure 1. For four states namely, $1^3\Sigma^-, 1^1\Delta$, $3^1\Pi$, and $3^3\Pi$, we detected weak van der Waals attractive interactions (ΔE_{vdw}) at interatomic distances $r_{vdw} \approx 4.35, 4.37, 3.30$, and 6.55 \AA with $\Delta E_{vdw} \approx -31, -49, -68$, and -63 cm^{-1} respectively.

B. ZnO^+ . As was mentioned in the introduction, experimental results on ZnO^+ are limited to a D_0^0 value and the ionization energy IE (ZnO). Applying the energy conservation relation $D_0^0(ZnO^+) - D_0^0(ZnO) + IE(ZnO) = IE(Zn) = 1.67 \pm 0.05^{10} - 1.61 \pm 0.04^{10} + 9.34 \pm 0.02^{10}$, we obtain $IE(Zn) = 9.40 \pm 0.11 \text{ eV}$, pretty consistent with the accurately determined ionization energy of Zn, $IE(Zn) = 9.394 \text{ eV}$.²²

Four asymptotic channels have been examined, that is, $Zn^+(^2S) + [O(^3P), O(^1D), O(^1S)]$ and $Zn^+(^2P) + O(^3P)$, giving rise to the following molecular $\Lambda-\Sigma$ states, respectively: $^2,4(\Sigma^-, \Pi)$, $^2(\Sigma^+, \Pi, \Delta)$, $^2\Sigma^+$, and $^2,4(\Sigma^+, \Sigma^-[2], \Pi[2], \Delta)$. We have calculated two bound PECs from the first channel ($X^2\Pi$, $a^4\Sigma^-$) (the other two are repulsive), all PECs form the next two channels, and four states from the fourth channel, namely, $2^2\Pi$, $1^4\Pi$, $3^2\Sigma^+$, and $2^2\Delta$. Figure 2 displays their MRCI+Q/A5 ζ PECs, and Table 3 collects all our numerical results including the theoretical RCCSD(T)/ \sim AQ ζ of Harrison et al.¹⁹ who examined the two states, $X^2\Pi$ and $2^2\Sigma^+$.

X $^2\Pi$. The leading equilibrium MRCI configuration and Mulliken densities of the ground state of ZnO^+ are,

$$|^2\Pi\rangle \approx 0.94|1\sigma^22\sigma^21\pi_x^11\pi_y^2\rangle$$

$$4s^{0.53}4p_z^{0.09}4p_x^{0.02}4p_y^{0.06}/_{Zn}2s^{1.93}2p_z^{1.43}2p_x^{0.97}2p_y^{1.90}/_O$$

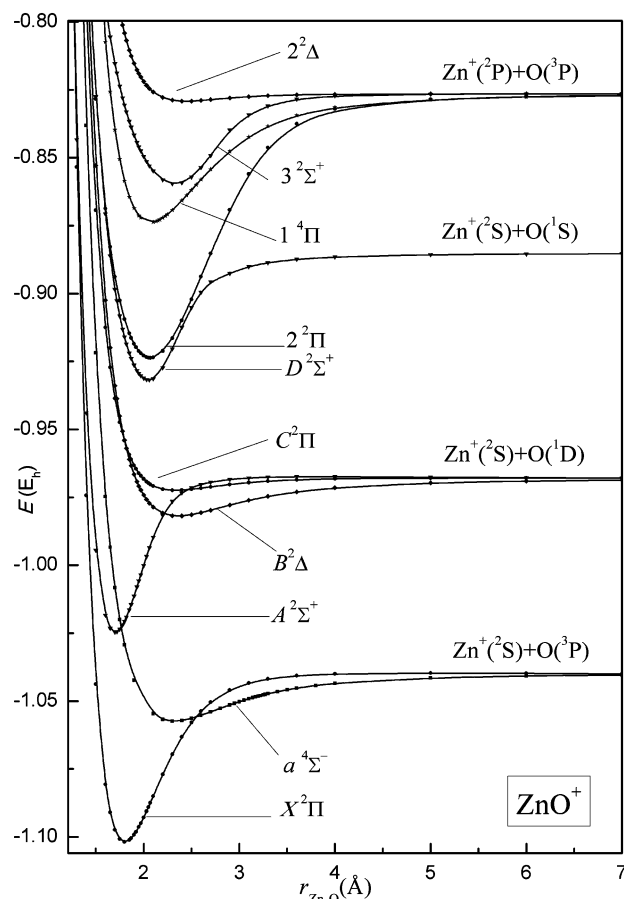


Figure 2. MRCI+Q/A5 ζ PECs of ZnO^+ . All energies are shifted by $+1852 E_h$.

with end products $Zn^+(^2S) + O(^3P; M_L = \pm 1)$. Clearly the bonding is the result of $\sim 0.35 e^-$ transfer from the $(4s4p_z)^{1.0}$ hybrid on Zn^+ to the singly occupied $2p_z$ orbital of the O atom; a total charge transfer of $\sim 0.30 e^-$ from Zn^+ to O is observed. The MRCI+DKH+Q(ACPF+DKH)[RCCSD(T)+DKH] bond distance and binding energy are, $r_e = 1.790(1.793)[1.786] \text{ \AA}$ and $D_0 = 1.63(1.60)[1.64] \text{ eV}$, with recommended values $r_e = 1.790 \pm 0.003 \text{ \AA}$ and $D_0 = 1.62 \pm 0.02 \text{ eV}$, respectively; see Table 3. The latter is in excellent agreement with the experimental value of $1.67 \pm 0.05 \text{ eV}$.¹⁰ Depending on the method, relativistic DKH effects reduce the bond distance by $0.010\text{--}0.016 \text{ \AA}$ and the binding energy by $0.01\text{--}0.04 \text{ eV}$. While harmonic frequencies are pretty stable in all methods of calculation from MRCI to RCCSD(T)+DKH ranging from $659\text{--}644 \text{ cm}^{-1}$ with a recommended value of $\omega_e = 650 \text{ cm}^{-1}$, the anharmonicity $\omega_e x_e$ is certainly underestimated at the coupled-cluster level. Finally the MRCI+DKH+Q(ACPF+DKH)[RCCSD(T)+DKH] ionization energy of ZnO , $IE(ZnO) = E(ZnO^+; X^2\Pi) - E(ZnO; X^1\Sigma^+) + \Delta\omega/2 = 9.14(9.20)[9.27] \text{ eV}$, pretty consistent with the experimental value of $9.34 \pm 0.02 \text{ eV}$.¹⁰

$a^4\Sigma^-$. This is the first excited state of ZnO^+ located close to 1.20 eV above the $X^2\Pi$ state. The main equilibrium MRCI configuration and the corresponding atomic Mulliken densities,

$$|a^4\Sigma^-\rangle \approx 0.90|1\sigma^22\sigma^23\sigma^11\pi_x^11\pi_y^1\rangle$$

$$4s^{1.01}4p_z^{0.05}4p_x^{0.01}4p_y^{0.01}/_{Zn}2s^{1.99}2p_z^{1.91}2p_x^{1.0}2p_y^{1.0}/_O$$

reveal a noncovalent interaction of $D_0 = 0.46 \pm 0.02 \text{ eV}$ at $r_e = 2.304 \pm 0.03 \text{ \AA}$, caused by a slight charge transfer of ~ 0.1

TABLE 3: Total Energies E (E_h), Bond Distances r_e (\AA), Dissociation Energies D_0 (eV), Harmonic Frequencies and Anharmonicity Corrections ω_e , $\omega_e x_e$ (cm^{-1}), Rotational-Vibrational Coupling Constants $\alpha_e \times 10^3$ (cm^{-1}), and Energy Separations T_0 (eV) of $^{64}\text{Zn}^{16}\text{O}^+$

method	$-E$	r_e	D_0	ω_e	$\omega_e x_e$	α_e	T_0
X $^2\Pi$							
MRCI	1853.06216	1.809	1.57	659	10.3	3.5	0.0
MRCI+Q	1853.1040	1.807	1.66	654	9.2	3.6	0.0
MRCI+DKH	1869.57936	1.793	1.54	662	10.2	4.1	0.0
MRCI+DKH+Q	1869.6221	1.790	1.63	660	9.8	4.0	0.0
ACPF	1853.10255	1.809	1.64	656	10.6	3.5	0.0
ACPF+DKH	1869.62058	1.793	1.60	659	10.4	4.0	0.0
RCCSD(T)	1853.12078	1.796	1.65	645		3.9	0.0
RCCSD(T) + DKH	1869.63938	1.786	1.64	644		4.1	0.0
RCCSD(T) ^a		1.798	1.66	644			
Expt. ^b			1.67 \pm 0.05				
a $^4\Sigma^-$							
MRCI	1853.00969	2.348	0.38	199	3.8	5.2	1.40
MRCI+Q	1853.0555	2.325	0.42	212	3.7	4.8	1.29
MRCI+DKH	1869.52861	2.332	0.39	204	3.8	5.1	1.35
MRCI+DKH+Q	1869.5753	2.307	0.44	217	3.7	4.7	1.25
ACPF	1853.05607	2.323	0.44	215	3.7	4.7	1.24
ACPF+DKH	1869.57591	2.304	0.46	221	3.7	4.6	1.19
RCCSD(T)	1853.07670	2.310	0.48	221	3.3	4.6	1.17
RCCSD(T) + DKH	1869.59653	2.301	0.50	229	3.3	4.6	1.14
A $^2\Sigma^+$							
MRCI	1852.99416	1.713	1.72	758	5.5	3.6	1.86
MRCI+Q	1853.0366	1.709	1.79	762	5.9	3.6	1.84
MRCI+DKH	1869.50681	1.700	1.57	754	5.1	3.8	1.98
MRCI+DKH+Q	1869.5501	1.696	1.68	758	5.6	3.8	1.97
ACPF	1853.03216	1.750	1.76	737	5.6		1.92
ACPF+DKH	1869.54569	1.727	1.54	781			2.03
RCCSD(T)	1853.05283	1.707	1.96	753	3.1	3.8	1.87
RCCSD(T) + DKH	1869.56707	1.697	1.81	755	3.2	4.1	1.98
RCCSD(T) ^a		1.708	1.74	759			1.99
B $^2\Delta$							
MRCI	1852.93433	2.384	0.32	181	3.82	5.8	3.45
MRCI+Q	1852.9812	2.360	0.34	192	3.69	5.4	3.31
C $^2\Pi$							
MRCI	1852.92510	2.352	0.08	124	5.60	12.6	3.70
MRCI+Q	1852.9726	2.330	0.12	146	5.23	9.9	3.55
D $^2\Sigma^+$							
MRCI	1852.87676	2.023	2.51	549	2.0	0.4	4.75
MRCI+Q	1852.9281	2.031	2.74	536	1.2	-0.1	4.70
2 $^2\Pi$							
MRCI	1852.87624	2.081	2.48	437	0.7	0.8	4.76
MRCI+Q	1852.9236	2.069	2.60	429	0.6	0.7	4.82
1 $^4\Pi$							
MRCI	1852.82735	2.084	1.16	372	3.6	3.6	6.08
MRCI+Q	1852.8737	2.075	1.26	380	3.4	3.5	6.17
3 $^2\Sigma^+$							
MRCI	1852.80786	2.399	0.646	295	1.2	0.1	6.61
MRCI+Q	1852.8596	2.330	0.885	320	0.7	-0.4	6.55
2 $^2\Delta$							
MRCI	1852.78491	2.524	0.03	97	6.71	16.3	7.51
MRCI+Q	1852.8291	2.438	0.07	127	6.72	12.4	7.45

^a Reference 19. ^b Reference 10. Guided ion beam mass spectrometry.

e^- from O to Zn^+ along the σ -frame. The $a^4\Sigma^-$ of ZnO^+ is calculated for the first time and of course is very difficult to be observed due to spin and Franck–Condon reasons; see Table 3 and Figure 2.

A $^2\Sigma^+$. The second excited state of ZnO^+ , located 2.00 eV above the X-state, is well bound with a recommended $D_0 = 1.75 \pm 0.05$ eV and $r_e = 1.700 \pm 0.03$ \AA , and a bond distance considerably shorter than all calculated states. As in the ground state, scalar relativity reduces the bond length by ~ 0.01 \AA , and the binding by ~ 0.15 eV. The main equilibrium MRCI configuration and atomic Mulliken populations are

$$|A^2\Sigma^+\rangle \approx 0.95|1\sigma^2 2\sigma^1 1\pi_x^2 1\pi_y^2\rangle \\ 4s^{0.22} 4p_z^{0.10} 4p_x^{0.09} 4p_y^{0.09} /_{\text{Zn}} 2s^{1.85} 2p_z^{0.82} 2p_x^{1.86} 2p_y^{1.86} /_{\text{O}}$$

with a Zn^+ to O charge transfer of 0.45 e^- . This is the only ZnO^+ state where a considerable charge transfer is recorded, the in situ atoms being $\text{Zn}^{1.5+}\text{O}^{0.5-}$. The symmetry of the end atoms $\text{Zn}^+(^2S) + \text{O}(^1D; M_L = 0)$, the main configuration and the corresponding populations, clearly show that the bonding is the result of ~ 0.7 e^- transfer from the $(4s4p_z)^{1.0}$ hybrid on Zn^+ to the $2p_z$ empty O orbital along the σ frame (2σ orbital), with a concomitant O to Zn back transfer of ~ 0.2 e^- along the π_p frame.

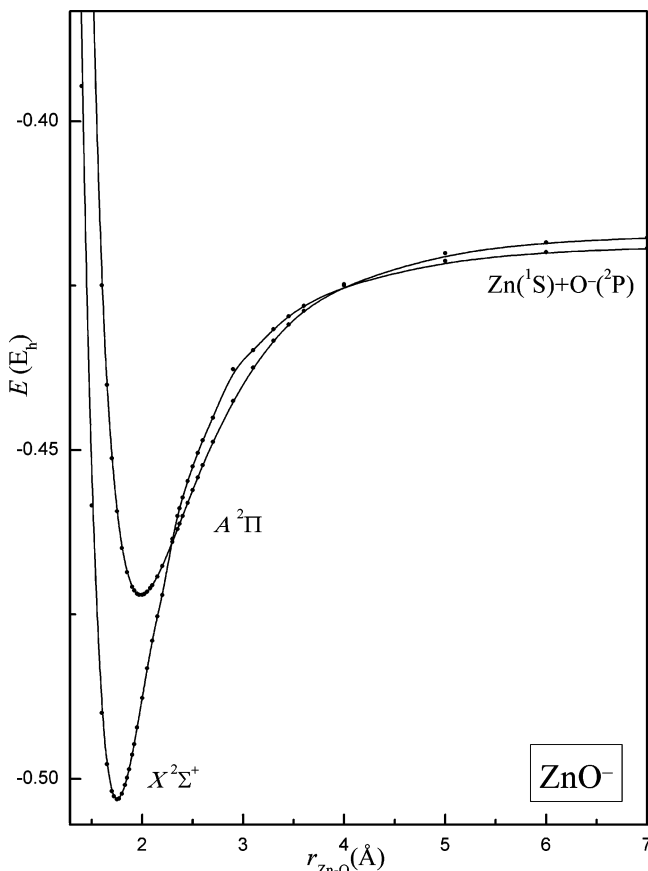


Figure 3. MRCI+Q/A5 ζ PECs of ZnO $^-$. All energies are shifted by +1853 E $_h$.

The most important MRCI configurations of the rest seven states and total Mulliken charges (q_{Zn}) are given below in ascending energy order; numerical results and PECs are shown in Table 3 and Figure 2.

TABLE 4: Total Energies E (E $_h$), Bond Distances r_e (Å), Dissociation Energies D_0 (eV), Harmonic Frequencies and Anharmonicity Corrections ω_e , $\omega_e x_e$ (cm $^{-1}$), Rotational-Vibrational Coupling Constants $\alpha_c \times 10^3$ (cm $^{-1}$). Energy Separations T_0 (eV) of $^{64}\text{Zn}^{16}\text{O}^-$.

method	$-E$	r_e	D_0	ω_e	$\omega_e x_e$	α_c	T_0
X$^2\Sigma^+$							
MRCI	1853.44839	1.753	2.24	704	6.1	4.1	0.0
MRCI+Q	1853.5031	1.752	2.25	696	6.7	4.3	0.0
MRCI+DKH	1869.97057	1.743	2.24	704	6.6	4.3	0.0
MRCI+DKH+Q	1870.0264	1.742	2.22	696	7.3	4.6	0.0
ACPF	1853.50640	1.755	2.12	689	7.1	4.5	0.0
ACPF+DKH	1870.02781	1.745	2.05	688	7.9	4.8	0.0
RCCSD(T)	1853.53122	1.755	2.21	677	7.9	4.4	0.0
RCCSD(T) + DKH	1870.05551	1.746	2.14	672		5.2	0.0
RCCSD(T) ^a		1.759	2.19	665			
Expt.			2.24 (± 0.05) ^b	625 \pm 40 ^b			
		1.753 ^c		650 \pm 50 ^c			
A$^2\Pi$							
MRCI	1853.41695	1.987	1.48	410	4.3	4.5	0.84
MRCI+Q	1853.4721	1.987	1.47	405	4.2	4.5	0.83
MRCI+DKH	1869.93907	1.987	1.40	400	4.3	4.6	0.84
MRCI+DKH+Q	1869.9953	1.987	1.39	395	4.2	4.6	0.83
ACPF	1853.47904	1.990	1.45	402	4.3	4.5	0.73
ACPF+DKH	1870.00098	1.991	1.38	392	4.3	4.7	0.73
RCCSD(T)	1853.50558	1.977	1.53	410	4.1	4.5	0.68
RCCSD(T) + DKH	1870.02948	1.975	1.45	401	4.1	4.6	0.69
RCCSD(T) ^a		1.984	1.50	407			0.71
Expt. ^c							0.73 \pm 0.07(= T_c)

^a Reference 19. ^b Reference 13, negative ion photoelectron spectroscopy (PES). ^c References 14 (PES) and 6 (rotational spectroscopy). $r_e = R(\text{X}^2\Sigma^+; \text{ZnO}) + 0.048(5) \text{ \AA}^{14} = 1.70474^6 + 0.048(5) = 1.7527 \pm 0.005 \text{ \AA}$.

$$\begin{aligned}
 |B^2\Delta\rangle &\approx \frac{1}{\sqrt{2}}|1\sigma^2 2\sigma^1(1\pi_x^1 2\pi_x^1 1\pi_y^2 - 1\pi_x^2 1\pi_y^1 2\pi_y^1)\rangle & (+0.95) \\
 |C^2\Pi\rangle &\approx 0.89|1\sigma^2 2\sigma^1 3\sigma^1 1\pi_x^1 1\pi_y^2\rangle & (+1.11) \\
 |D^2\Sigma^+\rangle &\approx \frac{1}{\sqrt{2}}|1\sigma^2 2\sigma^2 3\sigma^1(1\pi_x^2 - 1\pi_y^2)\rangle & (+1.02) \\
 |2^2\Pi\rangle &\approx 0.67|1\sigma^2 2\sigma^1 3\sigma^1 1\pi_x^1 1\pi_y^2\rangle & \\
 &+ 0.43|1\sigma^2 2\sigma^1 1\pi_x^1 1\pi_y^1 2\pi_y^1\rangle & (+1.04) \\
 |1^4\Pi\rangle &\approx 0.99|1\sigma^2 2\sigma^2 1\pi_x^1 1\pi_y^1 2\pi_y^1\rangle & (+0.87) \\
 |3^2\Sigma^+\rangle &\approx 0.50|1\sigma^2 2\sigma^1 1\pi_x^2 1\pi_y^2\rangle & \\
 &- 0.46|1\sigma^2 2\sigma^2 3\sigma^1(1\pi_x^2 + 1\pi_y^2)\rangle & (+0.98) \\
 |2^2\Delta\rangle &\approx 0.52|1\sigma^2 2\sigma^1(1\pi_x^1 2\pi_x^1 1\pi_y^2 + 1\pi_x^2 1\pi_y^1 2\pi_y^1)\rangle & (+0.94)
 \end{aligned}$$

With the exception of the $1^4\Pi$, where the in situ O atom loses $\sim 0.15 e^-$, in the rest of the states the oxygen atom remains practically neutral.

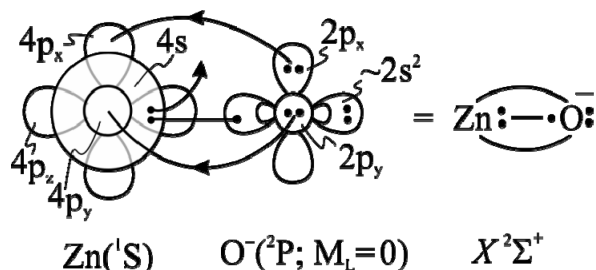
C. ZnO $^-$. For the ZnO $^-$ anion we have calculated the two states related to Zn($1S$) + O $^-(2P; M_L = 0, \pm 1)$ asymptote, $X^2\Sigma^+$ and $A^2\Pi$, respectively. Their MRCI+Q PECs are shown in Figure 3, and numerical results are listed in Table 4 along with experimental findings and the theoretical RCCSD(T)/ $\sim A4\zeta$ results of Harrison et al.¹⁹

The main MRCI equilibrium configurations, Mulliken distributions, and total charges on Zn (q_{Zn}) are

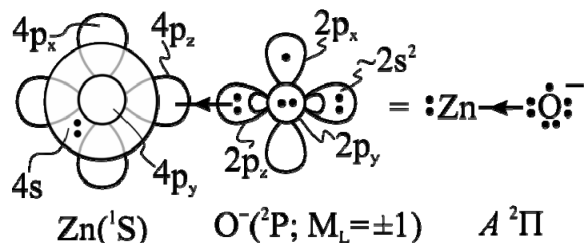
$$\begin{aligned}
 |X^2\Sigma^+\rangle &\approx 0.93|1\sigma^2 2\sigma^2 3\sigma^1 1\pi_x^2 1\pi_y^2\rangle & (-0.08) \\
 &4s^{1.30} 4p_z^{0.38} 4p_x^{0.18} 4p_y^{0.18} /_{Zn} 2s^{1.85} 2p_z^{1.44} 2p_x^{1.79} 2p_y^{1.79} /_O \\
 |A^2\Pi\rangle &\approx 0.94|1\sigma^2 2\sigma^2 3\sigma^2 1\pi_x^1 1\pi_y^2\rangle & (-0.34) \\
 &4s^{1.92} 4p_z^{0.34} 4p_x^{0.02} 4p_y^{0.04} /_{Zn} 2s^{1.95} 2p_z^{1.74} 2p_x^{0.99} 2p_y^{1.94} /_O
 \end{aligned}$$

The bonding is captured by the vBL diagrams in Schemes 5 and 6.

SCHEME 5



SCHEME 6



In the $X^2\Sigma^+$ state the three σ -electrons are coupled into a doublet, and $\sim 0.3 e^-$ are transferred from the $(4s4p_z)^2$ hybrid on Zn to the singly occupied $2p_z$ O orbital, concomitantly $\sim 0.4 e^-$ are moving from O^- to Zn along the π_p frame giving rise to two weak π bonds. This is also in agreement with the composition of the 2σ and 1π MRCI natural orbitals: $2\sigma \approx (0.59)4s^{\text{Zn}} - (0.75)2p_z^{\text{O}}$, $1\pi_{x(y)} \approx (0.84)2p_{x(y)}^{\text{O}} + (0.14)4p_{x(y)}^{\text{Zn}}$.

The bonding in the $A^2\Pi$ state is caused by a charge transfer of $\sim 0.3 e^-$ along the σ -frame from the $2p_z$ O orbital to the empty $4p_z$ Zn orbital. Indeed, $2\sigma \approx (0.77)4s^{\text{Zn}} - (0.23)4p_z^{\text{Zn}}$ and $3\sigma \approx (0.86)2p_z^{\text{O}} - (0.16)4p_z^{\text{Zn}}$.

At the MRCI+DKH+Q (ACPF+DKH) [RCCSD(T)+DKH] level the bond distance and binding energy of the $X^2\Sigma^+$ are 1.742 (1.745) [1.746] Å and 2.22 (2.05) [2.14] eV, respectively, in accord with the experimental values $r_e = 1.7527 \pm 0.005$ Å (see footnote of Table 4) and $D_0 = 2.24 \pm 0.05$ eV.¹³ Corresponding values for the $A^2\Pi$ state are 1.987 (1.991) [1.975] Å and 1.39 (1.38) [1.45] eV, with $T_0 = 0.83(0.73)[0.69]$ in agreement with the experimental value $T_e = 0.73 \pm 0.07$ eV. Our results are close to the RCCSD(T)/~AQ ζ results of Harrison et al.,¹⁹ see Table 4.

Finally, the MRCI+DKH+Q (ACPF+DKH) [RCCSD(T)+DKH] adiabatic electron affinity of ZnO is $\text{EA}(\text{ZnO}) = E(\text{ZnO}; X^1\Sigma^+) - E(\text{ZnO}^-; X^2\Sigma^+) + \Delta\omega/2 = 1.86$ (1.88) [2.04] eV, the coupled-cluster value being in accord with the experimental value(s) 2.088 ± 0.01 ,¹³ 2.087 ± 0.008 ,¹⁴ and 2.077 eV.¹⁵

4. Synopsis and Remarks

Complete PECs of 13, 10, and 2 states of ZnO, ZnO^+ , and ZnO^- , respectively have been constructed at the MRCI+Q/A5 ζ level of theory. The first 4 (ZnO), 3 (ZnO^+), and 2 (ZnO^-) states have been examined as well at the [MRCI, ACPF, RCCSD(T)] + DKH5 scalar relativity corrections. For all bound states we report total energies, binding energies, spectroscopic parameters, energy separations, and dipole moments (ZnO), whereas for the lowest states the bonding is discussed in some detail. All our results are in very good agreement with existing experimental findings.

The first 4 states of ZnO are fairly ionic with Mulliken Zn to O charge transfer of $0.50 - 0.65 e^-$, but the degree of ionicity decreases considerably for the higher states. In the ZnO^+ species

only in one state ($A^2\Sigma^+$) there is a significant charge transfer from Zn^+ to O ($\sim 0.5 e^-$), in the rest of the states in situ equilibrium atoms can be described by the formula Zn^+O . In the ZnO^- anion about $\sim 0.3 e^-$ are transferred from O^- to Zn in the first excited state ($A^2\Pi$).

As a final remark we can say that the calculated (recommended) dipole moment of the $X^1\Sigma^+$ of ZnO is $\mu_e = 5.3 \pm 0.1$ D, by far the highest of all calculated states, in harmony with the high ionicity of this state, $\text{Zn}^{0.65^+}\text{O}^{0.65^-}$.

References and Notes

- (1) Merer, A. J. *Annu. Rev. Phys. Chem.* **1989**, *40*, 407.
- (2) Harrison, J. F. *Chem. Rev.* **2000**, *100*, 679.
- (3) Miliordos, E.; Mavridis, A. *J. Phys. Chem. A* **2007**, *111*, 1953.
- (4) Miliordos, E.; Mavridis, A. *J. Phys. Chem. A* **2010**, *114* DOI: 10.1021/JP910218u.
- (5) Breslow, R. *Chem. Eng. News* **2003**, *81* (September), 86.
- (6) Zack, L. N.; Pulliam, R. L.; Ziurys, L. M. *J. Mol. Spectrosc.* **2009**, *256*, 186.
- (7) Anthrop, D. F.; Searcy, A. W. *J. Phys. Chem.* **1964**, *68*, 2335.
- (8) Prochaska, E. S.; Andrews, L. *J. Chem. Phys.* **1980**, *72*, 6782.
- (9) Wicave, B. G. *J. Chem. Phys.* **1983**, *78*, 6036.
- (10) Clemmer, D. E.; Dalleska, N. F.; Armentrout, P. B. *J. Chem. Phys.* **1991**, *95*, 7263.
- (11) Watson, L. R.; Thiem, T. L.; Dressler, R. A.; Salter, R. H.; Murad, E. *J. Phys. Chem.* **1993**, *97*, 5577.
- (12) Chertihin, G. V.; Andrews, L. *J. Chem. Phys.* **1997**, *106*, 3457.
- (13) Fancher, C. A.; de Clercq, H. L.; Thomas, O. C.; Robinson, D. W.; Bowen, K. H. *J. Chem. Phys.* **1998**, *109*, 8426.
- (14) Moravec, V. D.; Klopčič, S. A.; Chatterjee, B.; Jarrold, C. C. *Chem. Phys. Lett.* **2001**, *341*, 313.
- (15) Kim, J. H.; Li, X.; Wang, L.-S.; de Clercq, H. L.; Fancher, C. A.; Thomas, O. C.; Bowen, K. H. *J. Phys. Chem. A* **2001**, *105*, 5709.
- (16) Dolg, M.; Wedig, U.; Stoll, H.; Preuss, H. *J. Chem. Phys.* **1987**, *86*, 2123.
- (17) Boldyrev, A. I.; Simons, J. *Mol. Phys.* **1997**, *92*, 365.
- (18) Bauschlicher, C. W., Jr.; Partridge, H. *J. Chem. Phys.* **1998**, *109*, 8430.
- (19) Harrison, J. F.; Field, R. W.; Jarrold, C. C. *ACS Symp. Ser.* **2002**, *828*, 238.
- (20) Peterson, K. A.; Shepler, B. C.; Singleton, J. M. *Mol. Phys.* **2007**, *105*, 1139.
- (21) S. Boughdiri, S.; Tangour, B.; Teichteil, C.; Barthelat, J.; Leininger, T. *Chem. Phys. Lett.* **2008**, *462*, 18.
- (22) NIST Atomic Spectra Database (version 3.1.5), [Online]. Available: <http://physics.nist.gov/asd3> (Accessed June 28, 2009). National Institute of Standards and Technology, Gaithersburg, MD, 2009.
- (23) Balabanov, N. B.; Peterson, K. A. *J. Chem. Phys.* **2005**, *123*, 064107.
- (24) Dunning, T. H., Jr. *J. Chem. Phys.* **1989**, *90*, 1007. Kendall, R. A.; Dunning, T. H., Jr.; Harrison, R. J. *J. Chem. Phys.* **1992**, *96*, 6796.
- (25) Raghavachari, K.; Trucks, G. W.; Pople, J. A.; Head-Gordon, M. *Chem. Phys. Lett.* **1989**, *157*, 479. Watts, J. D.; Bartlett, R. J. *J. Chem. Phys.* **1993**, *98*, 8718. Knowles, P. J.; Hampel, C.; Werner, H.-J. *J. Chem. Phys.* **1993**, *99*, 5219. *ibid* **2000**, *112*, 3106E.
- (26) Werner, H.-J.; Knowles, P. J. *J. Chem. Phys.* **1988**, *89*, 5803. Knowles, P. J.; Werner, H.-J. *Chem. Phys. Lett.* **1988**, *145*, 514.
- (27) Douglas, M.; Kröll, N. M. *Ann. Phys.* **1974**, *82*, 89.
- (28) Hess, B. A. *Phys. Rev. A: At. Mol. Opt. Phys.* **1985**, *32*, 756. *ibid.* **1986**, *33*, 3742.
- (29) Langhoff, S. R.; Davidson, E. R. *Int. J. Quantum Chem.* **1974**, *8*, 61. Davidson, E. R.; Silver, D. W. *Chem. Phys. Lett.* **1977**, *52*, 403.
- (30) Gdanitz, R. J.; Ahlrichs, R. *Chem. Phys. Lett.* **1988**, *143*, 413. Werner, H.-J.; Knowles, P. J. *Theor. Chim. Acta* **1990**, *78*, 175.
- (31) Werner, H.-J.; Knowles, P. J.; Lindh, R.; Manby, F. R.; Schütz, M.; Celani, P.; Korona, T.; Mitrushenkov, A.; Rauhut, G.; Adler, T. B.; Amos, R. D.; Bernhardsson, A.; Berning, A.; Cooper, D. L.; Deegan, M. J. O.; Dobbyn, A. J.; Eckert, F.; Goll, E.; Hampel, C.; Heter, G.; Hrenar, T.; Knizia, G.; Köppl, C.; Liu, Y.; Lloyd, A. W.; Mata, R. A.; May, A. J.; McNicholas, S. J.; Meyer, W.; Mura, M. E.; Nicklass, A.; Palmieri, P.; Pflüger, K.; Pitzer, R.; Reiher, M.; Schumann, U.; Stoll, H.; Stone, A. J.; Tarroni, R.; Thorsteinsson, T.; Wang, M.; Wolf, A. MOLPRO, version 2006.1, a package of ab initio programs; see <http://www.molpro.net>.
- (32) Bunge, C. E.; Barrientos, J. A.; Bunge, A. V. *At. Data Nucl. Data Tables* **1993**, *53*, 113.
- (33) Tzeli, D.; Mavridis, A. *J. Chem. Phys.* **2003**, *118*, 4984.